Interactions between Poloxamers in Aqueous Solutions: Micellization and Gelation Studied by Differential Scanning Calorimetry, Small Angle X-ray Scattering, and Rheology

Franck Artzner,[†,‡] Sandrine Geiger,[†] Audrey Olivier,[†] Cécile Allais,[†] Stéphanie Finet,[§] and Florence Agnely*[,†]

UMR CNRS 8612, Univ Paris-Sud, Faculté de Pharmacie, 5 rue JB Clément, 92296 Châtenay-Malabry Cedex, France, UMR CNRS 6626, Université Rennes I, 35042 Rennes Cedex, France, and E.S.R.F., 6 rue Jules Horowitz, BP 220, 38043 Grenoble cedex 9, France

Received September 7, 2006. In Final Form: January 22, 2007

Poloxamers F88 ($EO_{97}PO_{39}EO_{97}$) and P85 ($EO_{27}PO_{39}EO_{27}$) are triblock copolymers of ethylene oxide (EO) and propylene oxide (PO), which have the same hydrophobic PO block. We studied aqueous solutions of these two copolymers by the conjoint use of differential scanning calorimetry (DSC), rheology, and small-angle X-ray scattering (SAXS). The results showed that the temperature-induced micellization of aqueous solutions of F88 and P85 was a progressive process followed by gelation for sufficiently concentrated samples. Gelation was due to the ordered packing of micelles under a hexagonal compact (HC) structure for P85 and a body-centered cubic (BCC) phase for F88. Importantly, the phase diagram of F88/P85 mixtures in water was elucidated and showed the destabilization of the HC phase upon addition of small amounts of F88.

Introduction

Amphiphilic triblock copolymers composed of poly(ethylene oxide) (PEO) and poly(propylene oxide) (PPO), often denoted PEO−PPO−PEO or $(EO)_a(PO)_b(EO)_a$, are commercially available products known as Pluronics or Poloxamers. These copolymers find various applications in detergency, foaming, dispersion stabilization, and emulsification.[1] In the pharmaceutical field, they are used for drug solubilization and for controlled release. The work in this field has recently been reviewed.[2,3] Over the past decade, many studies were devoted to the properties of poloxamers in aqueous solution. At low temperature and in dilute solutions, poloxamer molecules exist as unimers.[4−6] With an increase of solution temperature or polymer concentration, micellization occurs and a critical micellar concentration (cmc) and a critical micellar temperature (cmt) can be defined.[4,7−17] The cmc and the cmt were mainly studied by differential scanning calorimetry (DSC)[4,13−17] and fluorescence or UV probe spectroscopy.[9−12] Aggregation arises as a result of the dehydration of the PPO moieties leading to the formation of micelles, with a core dominated by PPO and a water swollen corona dominated by PEO.[4,6,18−25] The size, aggregation number (i.e., the average number of poloxamer molecules involved in a micelle), and micelle structure and hydration were mostly studied by small-angle neutron scattering,[4−6,18−21] light scattering,[4,7] and electron spin resonance.[22−25] Moreover, at high concentration, some poloxamer solutions exhibit a huge increase of viscosity with temperature, leading to a thermoreversible gelation. Rheology experiments allow the determination of the sol−gel transition temperature, T_{gel}, which is related to a dramatic change in the sample rheological properties. Below T_{gel}, the poloxamer solution behaves as a viscous liquid with a Newtonian behavior, whereas above T_{gel}, a shear-thinning behavior of the gel is observed.[26−31]

* To whom correspondence should be addressed. Telephone: 33 1 46 83 56 26. Fax: 33 1 46 83 58 82. E-mail: florence.agnely@u-psud.fr.

† UMR CNRS 8612, Univ Paris-Sud.

‡ UMR CNRS 6626, Université Rennes I.

§ E.S.R.F.

(1) Schmolka, I. R. *Am. Perfum. Cosmet.* **1967**, *82*, 25−30.

(2) Adams, M. L.; Lavasanifar, A.; Kwon, G. S. *J. Pharm. Sci*. **2003**, *92* (7), 1343−1355.

(3) Kabanov, A. V.; Batrakova, E. V.; Alakhov, V. Y. *J. Controlled Release* **2002**, *82*, 189−212.

(4) Wanka, G.; Hoffmann, H.; Ulbricht, W. *Macromolecules* **1994**, *27*, 4145−4159.

(5) Aswal, V. K.; Goyal, P. S.; Kohlbrecher, J.; Bahadur, P. *Chem. Phys. Lett.* **2001**, *349*, 458−462.

(6) Mortensen, K.; Pedersen, J. S. *Macromolecules* **1993**, *26*, 805−812.

(7) Altinok, H.; Yu, G.-E.; Nixon, S. K.; Gorry, P. A.; Attwood, D.; Booth, C. *Langmuir* **1997**, *13*, 5837−5848.

(8) Yu, G.-E.; Altinok, H.; Nixon, S. K.; Booth, C.; Alexandridis, P.; Hatton, T. A. *Eur. Polym. J.* **1997**, *33*, 673−677.

(9) Gaisford, S.; Beezer, A. E.; Mitchell, J. C.; Bell, P. C.; Fakorede, F.; Finnie, J. K.; Williams, S. T. *Int. J. Pharm.* **1998**, *174*, 39−46.

(10) Batrakova, E. V.; Lee, S.; Li, S.; Venne, A.; Alakhov, V. Y.; Kabanov, A. V. *Pharm. Res.* **1999**, *16*, 1375−1381.

(11) Alexandridis, P.; Holzwarth, J. F.; Hatton, T. A. *Macromolecules* **1994**, *27*, 2414−2425.

(12) Wang, R.; Knoll, H.; Rittig, F.; Kärger, J. *Langmuir* **2001**, *17*, 7464−7467.

(13) Amstrong, J. K.; Parsonage, J.; Chowdhry, B.; Leharne, S.; Mitchell, J.; Beezer, A.; Löhner, K.; Laggner, P. *J. Phys. Chem.* **1993**, *97*, 3904−3909.

(14) Beezer, A. E.; Loh, W.; Mitchell, J. C.; Royall, P. G.; Smith, D. O.; Tute, M. S.; Armstrong, J. K.; Chowdhry, B. Z.; Leharne, S. A.; Eagland, D.; Crowther, N. J. *Langmuir* **1994**, *10*, 4001−4005.

(15) Hecht, E.; Hoffmann, H. *Colloids Surf., A* **1995**, *96*, 181−197.

(16) Paterson, I.; Armstrong, J.; Chowdhry, B.; Leharne, S. *Langmuir* **1997**, *13*, 2219−2226.

(17) Michels, B.; Waton, G.; Zana, R. *Colloids Surf., A* **2001**, *183−185*, 55−66.

(18) Yang, L.; Alexandridis, P.; Steytler, D. C.; Kositza, M. J.; Holzwartz, J. F. *Langmuir* **2000**, *16*, 8555−8561.

(19) Jain, N. J.; Aswal, V. K.; Goyal, P. S.; Bahadur, P. *Colloids Surf., A* **2000**, *173*, 85−94.

(20) Pederson, J. S.; Gertensberg, M. C. *Colloids Surf., A* **2003**, *213*, 175−187.

(21) Liao, C.; Choi, S.-M.; Mallamace, F.; Chen, S.-H. *J. Appl. Crystallogr*. **2000**, *33*, 677−681.

(22) Caragheorgheopol, A.; Caldararu, H.; Dragutan, I.; Joela, H.; Brown, W. *Langmuir* **1997**, *13*, 6912−6921.

(23) Caragheorgheopol, A.; Schlick, S. *Macromolecules* **1998**, *31*, 7736−7745.

(24) Zhou, L.; Schlick, S. *Polymer* **2000**, *41*, 4679−4689.

(25) Guo, C.; Wang, J.; Liu, H.-Z.; Chen, J.-Y. *Langmuir* **1999**, *15*, 2703−2708.

(26) Miller, S. C.; Drabik, B. R. *Int. J. Pharm.* **1984**, *18*, 269−276.

(27) Lenaert, V.; Triqueneaux, C.; Quarton, M.; Rieg-Falson, F.; Couvreur, P. *Int. J. Pharm.* **1987**, *39*, 121−127.

(28) Dumortier, G.; Grossiord, J. L.; Zuber, M.; Couarraze, G.; Chaumeil, J. C. *Drug development and Industrial Pharmacy* **1991**, *17*, 1255−1265.

10.1021/la062622p CCC: $37.00
Published on Web 03/22/2007

These thermoreversible poloxamer gels are of great potential interest in the pharmaceutical field, as they could be used for the controlled delivery of drugs. Indeed, they could be administered conveniently in liquid form (for instance, via syringes) and then gel in situ, provided the sol−gel transition temperature is lower than the body temperature.[28,32,33] Several mechanisms were proposed to describe this thermal gelation, the most commonly admitted being a "hard sphere crystallization" of the micelles under a cubic phase.[4,34] This crystallization was evidenced by small-angle X-ray scattering[35] or small-angle neutron scattering experiments,[4,36] and indexation of the Bragg diffraction peaks allowed identification of the different phases. For F88 and P85 poloxamers, a body-centered cubic (BCC) phase was reported.[36,37] According to Liu and Chu,[38,39] a face-centered cubic (FCC) structure is obtained for poloxamer F127 for polymer concentrations ranging between 20 and 40%, whereas at a higher concentration (50%), a BCC packing of micelles is observed.

Besides, extensive work has been done to elucidate the rich phase behaviors of poloxamers in mixed solvents.[40−42] However, information on the mixture of two poloxamers in water is still missing. Such systems are of great academic and practical interest. Indeed, they would provide a more extensive understanding of the relationship between the association properties and the molecular architecture of the copolymers. Moreover, the composition of the mixture might be an alternative way to modulate the gelation temperature and the structure of the system to meet the requirements of specific applications (for instance, body temperature in pharmaceutical or medical applications). Gaisford et al.[43] investigated the influence of varying polymeric mass on the cooperative or noncooperative binding of poloxamer binary mixtures in dilute solutions by UV spectroscopy. Mixtures of poloxamer F127 and a triblock copolymer composed of two blocks of poly(ethylene oxide) surrounding a central block of poly(butylene oxide) were studied by Liu et al.[39,44] However, based on our knowledge, there is no study on the structure and rheological properties of poloxamer mixtures in the gel state.

In the present work, we report on both the micellization and the gelation processes for two poloxamers (F88 and P85) having the same PPO block but different PEO blocks. These poloxamers were studied alone in water and as binary mixtures in water by the conjoint use of three techniques: small-angle X-ray scattering (SAXS), differential scanning calorimetry (DSC), and rheology.

Materials and Methods

Copolymers. Poloxamer samples (F88 and P85) were kindly provided by BASF and were used without further purification. F88 has a molecular weight of 10 800 g·mol^{-1} and corresponds to EO_{97}-$PO_{39}EO_{97}$, whereas P85 has a molecular weight of 4600 g·mol^{-1} and corresponds to $EO_{27}PO_{39}EO_{27}$. These are nominal values. Previous studies on poloxamers have shown that these copolymers, which are synthesized via anionic polymerization, are in fact heterogeneous in composition and may contain, for instance, some diblock impurities.[4,45] This variability in composition depends on the supplier. As many other authors working on poloxamers, we chose to study nonpurified samples to remain close to the industrial use of these polymers.

Solution and Mixture Preparation. Poloxamer aqueous solutions were prepared according to the so-called "cold method". The polymer was dissolved in cold ($T = 4$ °C) doubly permuted water under gentle magnetic stirring. After dissolution, each solution was equilibrated overnight at $T = 4$ °C. Poloxamer stock solutions were thus prepared at concentrations of 30% (w/w) or 35% (w/w). Samples with concentrations ranging between 5% and 30% were then obtained by proper dilution of the stock solutions with doubly permuted cold water. Poloxamer mixtures were prepared by mixing varying amounts of F88 and P85 solutions at the same concentrations. All systems were equilibrated at least 18 h at $T = 4$ °C before use.

Rheology. Rheological measurements were performed with a Carri Med CSL 100 rheometer using a cone-plate geometry (diameter 2 cm, angle 2°, gap between the plate and the truncated cone 54 μm). A solvent trap was used to prevent water evaporation during the experiments. The viscosity of the samples was recorded under an imposed shear rate of 5 s^{-1} as temperature was increased at a rate of 1 °C/min. The temperature range investigated was ±10 °C around the sol−gel transition temperature (T_{gel}). This ramp allowed the samples to be at their thermal equilibrium. It may, however, be too fast for the samples to reach their mechanical equilibrium at each temperature. No temperature-dependent gap correction was applied during this temperature ramp.

DSC. DSC experiments were performed with a Perkin-Elmer DSC 7 apparatus. Approximately 5 mg of poloxamer aqueous solution was placed in sealed aluminum pans. Prior any measurement, the sample was submitted to the following thermal cycle: heating from 0 to 50 °C, cooling from 0 to −80 °C, and then heating from −80 to 0 °C at a rate of 5 °C/min. DSC traces were then recorded as the temperature increased from 0 to 50 °C at a rate of 5 °C/min with an empty pan as a reference.

SAXS. X-ray diffraction experiments were performed at the High Brilliance Beam Line (ID2)[46] at the European Synchrotron Radiation Facility (ESRF) in Grenoble, France. The undulator X-ray beam (wavelength 0.99 Å) was selected by a channel-cut Si(111) crystal and focused by a rhodium-coated toroïdal mirror. The beam size defined by the collimated slits was 0.2 mm × 0.2 mm. The detector was an image-intensified charge-coupled device (CCD) camera. The sample-to-detector distance was 3.00 m. The beam-stop size was 9 mm × 6 mm (h×v). Low diffuse scattering arising from the direct beam was not completely eliminated and produced a small-angle scattering below 0.03 Å^{-1}. In these conditions, the practical q-range was larger than 0.01−0.2 Å^{-1} and the experimental resolution was better than 0.0008 Å^{-1} (fwhm). Samples were loaded in thin Lindman glass capillaries (diameter 1.6 ± 0.1 mm and thickness 10 μm) (GLAS, Muller, Berlin, Germany) sealed with wax. They were introduced into a homemade capillary holder, which allows maintenance of 20 capillaries all together at a controlled temperature or application of a determined temperature ramp from 20 up to 50 °C in 90 min via a computer.[47] The high flux led us to decrease the acquisition time to 300 ms. High statistic SAXS patterns were

(29) Cho, C.-W.; Shin, S.-C.; Oh, I.-J. *Drug Dev. Ind. Pharm.* **1997**, *23*, 1227−1232.
(30) Cabana, A.; Aït-Kadi, A.; Juhàsz, J. *J. Colloid Interface Sci.* **1997**, *190*, 307−312.
(31) Edsman, K.; Carlfors, J.; Petersson, R. *Eur. J. Pharm. Sci.* **1998**, *6*, 105−112.
(32) Veyries, M. L.; Couarraze, G.; Geiger, S.; Agnely, F.; Massias, L.; Kunzli, B.; Faurisson, F.; Rouveix, B. *Int. J. Pharm.* **1999**, *192*, 183−193.
(33) Koffi, A. A.; Agnely, F.; Ponchel, G.; Grossiord, J. L. *Eur. J. Pharm. Sci.* **2006**, *276*, 328−335.
(34) Wanka, G.; Hoffmann, H.; Ulbricht, W. *Colloid Polym. Sci.* **1990**, *268*, 101−117.
(35) Alexandridis, P. *Macromolecules* **1998**, *31*, 6935−6942.
(36) Mortensen, K.; Brown, W.; Nordén, B. *Phys. Rev. Lett.* **1992**, *68*, 2340−2343.
(37) Mortensen, K. *Europhys. Lett.* **1992**, *19*, 599−604.
(38) Wu, C.; Liu, T.; Chu, B. *J. Non-Cryst. Solids* **1998**, *235*−*237*, 605−611.
(39) Liu, T.; Chu, B. *J. Appl. Crystallogr.* **2000**, *33*, 727−730.
(40) Svensson, B.; Olsson, U.; Alexandridis, P. *Langmuir* **2000**, *16*, 6839−6846.
(41) Ivanova, R.; Alexandridis, P.; Lindman, B. *Colloids Surf., A* **2001**, *183*−*185*, 41−53.
(42) Ivanova, R.; Lindman, B.; Alexandridis, P. J. *Colloid Interface Sci.* **2002**, *252*, 226−235.
(43) Gaisford, S.; Beezer, A. E.; Mitchell, J. C. *Langmuir* **1997**, *13*, 2606−2607.
(44) Liu, T.; Nace, V. M.; Chu, B. *Langmuir* **1999**, *15*, 3109−3117.
(45) Batsberg, W.; Nodni, S.; Trandum, C.; Hvidt, S. *Macromolecules* **2004**, *37*, 2965−2971.
(46) Narayanan, T.; Diat, O.; Boesecke, P. *Nucl. Instrum. Methods Phys. Res., Sect. A* **2001**, *465*, 1005−1009.
(47) Valéry, C.; Artzner, F.; Robert, B.; Gulick-Krziwicki, T.; Keller, G.; Grabielle-Madelmont, C.; Torres, M.-L.; Calvo, P.; Cherif-Cheikh, R.; Narayanan, T.; Paternostre, M. *Biophys. J.* **2004**, *86*, 2484−2501.

obtained by adding 10 frames of 300 ms each acquired in translated positions to reduce the degradation of the samples that appears for exposure longer than 3 s with these samples. The data treatments and interpretations did not require background subtraction or normalization. Only raw data are shown.

Results and Discussion

1. Micellization. Samples of P85 and F88 with concentrations ranging between 5 and 30% (w/w) were studied by DSC. Upon temperature increase, micellization of poloxamer solutions appears on thermograms as a broad and asymmetric endothermic peak spreading over approximately 10 °C for F88 and 15 °C for P85. An example of a DSC scan is given in Figure 1, which displays the thermogram obtained with P85 at a concentration $C = 20\%$ (w/w). Two temperatures could be defined from the thermograms (see Figure 1): T_{onset} and T_{end}, the temperature of the beginning of poloxamer association and the temperature of the end of the micellization process, respectively. T_{onset} corresponds to the cmt (critical micellization temperature) of the poloxamer solution. For P85, at $C = 20\%$, $T_{onset} = 18$ °C and $T_{end} = 34$ °C. Table 1 recapitulates the values of T_{onset} and T_{end} obtained for the different poloxamer solutions studied. On the thermogram, the peak area can be described as the micellization enthalpy, which was shown to be strongly correlated to the PPO block size.[4,15,45] From our experiments, it was possible to calculate the average micellization enthalpy per mole of PO monomer, $\Delta H_{/PO}$. We obtained $\Delta H_{/PO} = 2.1$ kJ/mol$_{PO}$ for F88 and $\Delta H_{/PO} = 4.4$ kJ/mol$_{PO}$ for P85. These values are of the same order of magnitude. Beezer et al.[14] reported a value of 5 kJ/mol for the theoretical micellization enthalpy per propylene oxide in the absence of any EO unit, which is in good agreement with our results. For the further development of this article, we made the assumption that beyond the end of the micellization process, that is, at T_{end} and above, all poloxamer molecules have been transferred into micelles (the number of unimers is negligible). This assumption was used to determine the micelle structure in the gel state (see section 5) and is validated by the previous results of Brown et al.[48] These authors have studied a 4.8% P85 aqueous solution at temperatures ranging between 15 °C and 50 °C by dynamic light scattering. They showed that the micellization occurred gradually over a temperature range in the vicinity of 25 °C and that a mixture of unimers and micelles coexisted below 40 °C, whereas at 40 °C and above, only the micellar form existed. This temperature of 40 °C corresponds to the value of T_{end} obtained with our P85 solution at $C = 5\%$ (see Table 1).

Micellization of the poloxamer solution also induced a viscosity increase, which could be recorded with the Carrimed CSL 100 rheometer only for sufficiently concentrated samples. For instance, for P85 at $C = 25\%$, the viscosity raised from 0.03 to 1 Pa·s when temperature was increased from 30 to 45 °C. The viscosity of simple liquids (for instance, water or most polymer solutions) usually decreases with temperature due to the weakening of molecular interactions. The viscosity increase observed in our systems was macroscopic evidence of the poloxamer temperature-induced association and of the growing interactions between micelles. However, this kind of experiments was not sensible enough to detect the onset of micellization.

The evolution of the X-ray patterns as a function of temperature also provides information on the micellization process. Figure 2 displays the SAXS intensity profiles as a function of the scattering vector obtained for the P85 solution at $C = 20\%$ for

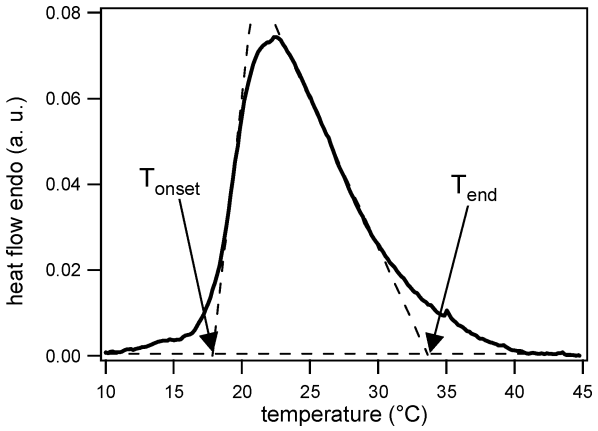

Figure 1. DSC trace of the P85 aqueous solution, $C = 20\%$ (w/w). Endothermic peak of micellization and definition of T_{onset} and T_{end}.

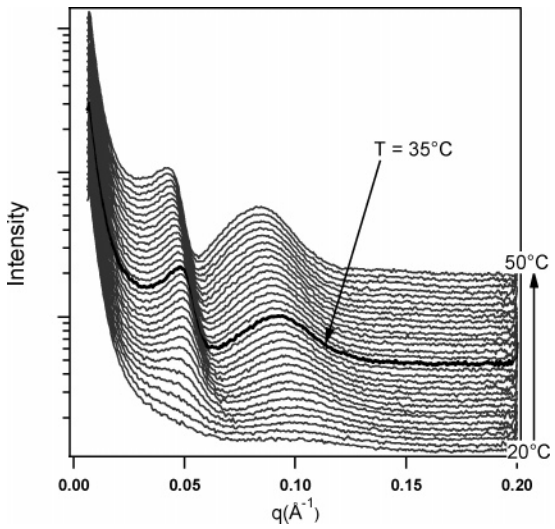

Figure 2. X-ray profiles of the P85 aqueous solution, $C = 20\%$ (w/w) at temperatures ranging between 20 and 50 °C.

temperatures ranging between 20 and 50 °C. At $T = 20$ °C, which is the lowest temperature investigated by SAXS, one can observe two broad peaks. These peaks could be attributed to the presence of micelles, which are assumed to be spherical. At $T = 20$ °C, micelles already existed in solution as $T_{onset} = 18$ °C for this system. The intensities of the two peaks increased with temperature up to $T = 34$ °C and then remained quasi-constant at higher temperature, which means that the process of micellization is completed. This temperature corresponds to T_{end}, denoting a good agreement between the SAXS and the DSC experiments.

2. Micelle Structure in Solution. In the case of n identical spherical particles, the scattered intensity $I(q)$ in SAXS experiments is given by eq 1:

$$I(q) \propto P(q)\, S(q) \tag{1}$$

where q is the scattering vector ($q = 4\pi/\lambda \sin\theta$, where 2θ is the scattering angle and λ is the the wavelength of the incident beam), $S(q)$ is the structure factor which reflects the interparticle interactions, and $P(q)$ is the particle form factor. In the first approximation, for spherical particles with a radius R with a sharp interface, the form factor is given by eq 2:

$$P(q) \propto \left[3\Delta\rho\left(\frac{4\pi R^3}{3}\right)\frac{\sin(qR) - qR\cos(qR)}{(qR)^3}\right]^2 \tag{2}$$

(48) Brown, W.; Shillén, K.; Almgren, M.; Hvidt, S.; Bahadur, P. *J. Phys. Chem.* **1991**, *95*, 1850−1858.

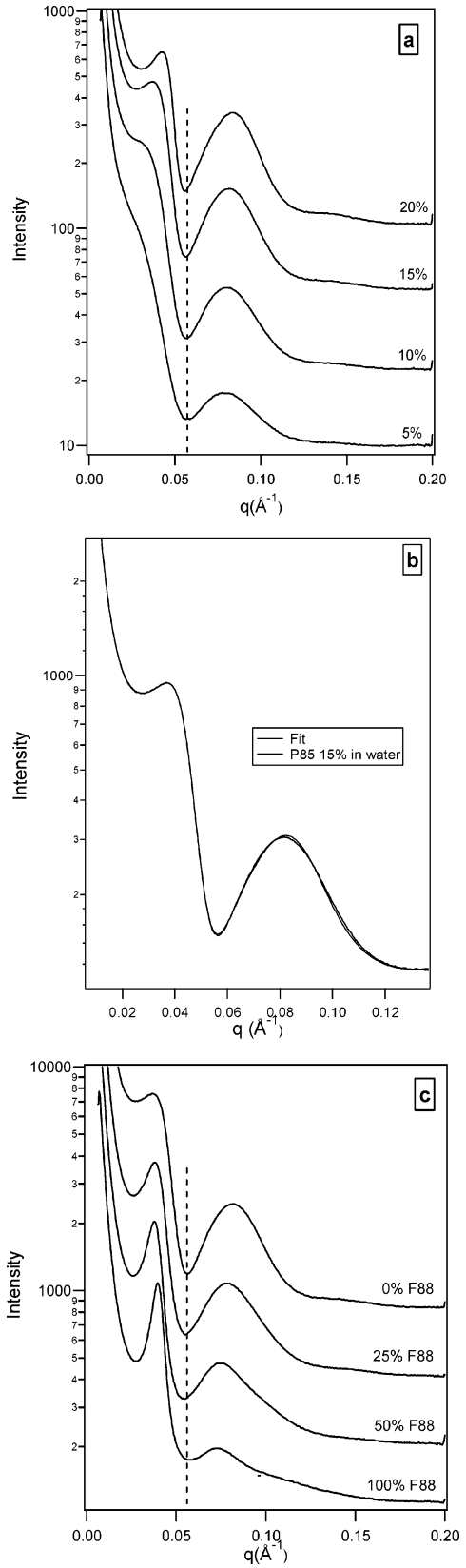

Figure 3. (a) X-ray profiles of the P85 aqueous solutions at concentrations $C = 5\%$ (w/w), $C = 10\%$ (w/w), $C = 15\%$ (w/w), and $C = 20\%$ (w/w) and at $T = 50$ °C. (b) X-ray profile of the P85 aqueous solution at $C = 15\%$ (w/w) and $T = 50$ °C, and fit of the experimental data (form factor: core−shell model with a low polydispersity, structure factor: hard sphere model). (c) X-ray profiles of F88/P85 aqueous solutions with various amounts of F88 (0%, 25%, 50%, 100%) at total polymer concentration $C = 15\%$ (w/w) and $T = 50$ °C. The dotted lines serve as a guide for the eyes.

where $\Delta\rho$ is the difference in electron densities between the particle and the solvent. In the case of poloxamer micelles, the interface could be either the core−shell PEO/POP interface or the external PEO/water interface. The first zero of $P(q)$ is obtained for $qR = 4.5$ and corresponds to a deep minimum of the scattered intensity, independently of the particle concentration (provided the particle size does not vary with concentration). Moreover, the high statistic data (Figure 3) were fitted using a core−shell model with a low polydispersity as a form factor[49] and using a hard sphere model as a structure factor.

Figure 3a displays the variations of the scattered intensity versus q at $T = 50$ °C for different P85 concentrations, and Figure 3b gives an example of the fits obtained. Similar X-ray profiles were also reported by Glatter et al. for P85.[50] One can note the presence of two minima in the SAXS profiles. The position and the depth of the first minimum (at low q values) depend on poloxamer concentration, whereas the position of the second one, which is a pronounced minimum, remains unchanged when the poloxamer concentration is increased. The first minimum is thus related to a minimum of the structure factor $S(q)$, while the second minimum can be attributed to a zero of the particle form factor $P(q)$. From the position of this second minimum, it was possible to calculate the mean micelle radius R. At $T = 50$ °C, $R = 80 \pm 2$ Å and is independent of poloxamer concentration. This is confirmed by a detailed fit analysis which indicates a very low polydispersity (6−8%), a quasi-constant external radius of the micelle (69−71 Å), and an increase of the evaluated hard sphere volume fraction, which is proportional to the experimental volume fraction. The values of the radius, which are slightly model dependent, are similar to that of the hydrodynamic radius obtained for P85 micelles at $T = 50$ °C by dynamic light scattering by Brown et al.[48] This indicates that the electron density interface is not the core−shell PEO/POP interface but the external PEO/water interface. The position of the first maximum (at low $q <$ 0.05 Å^{-1}) is shifted to higher q values, and its height is increased with increasing concentration. This evolution is due to growing pair interaction between micelles as the mean distance between micelles decreases. From Figure 2, it can also be deduced that the micellar radius increases with temperature (the position of the second minimum is shifted to lower q values). This is in agreement with already reported results,[4,18] and this effect is due to the progressive dehydration of poloxamer chains with temperature.[25] The poloxamer molecules thus become more hydrophobic and are transferred into growing micelles.

Figure 3c displays the variations of the SAXS intensity profiles with increasing F88 ratios for F88/P85 mixtures at a constant total polymer concentration $C = 15\%$. The position of the second minimum is independent of the system composition, denoting that the micellar radius is the same for all these systems ($R = 80 \pm 2$ Å). A more detailed fit study confirms the constant radius (66−72 Å) and the micelle interaction increase when exchanging P85 with F88. Interestingly, the micelle radius obtained from the form factor is constant while the interaction equivalent hard sphere radius measured from the structure factor slightly increases (10%). These results indicate a complex conformation behavior of the PEO blocks in poloxamer mixtures.

3. Gelation. With sufficiently concentrated samples, a reversible gelation was observed above the sol−gel transition temperature, T_{gel}. Below T_{gel}, the samples behaved as viscous solutions, whereas above T_{gel}, they were gels and an infinite

(49) Hayter, J. B. In *Physics of Amphiphiles-Micelles, Vesicles, and Microemulsions*; DeGiorgio, V., Corti, M., Eds.; North Holland: Amsterdam, 1983; pp 59−93. Kline, S. R. *J. Appl. Crystallogr.* **2006**, *39*, 895−900.

(50) Glatter, O.; Scherf, G.; Schillén, K.; Brown, W. *Macromolecules* **1994**, *27*, 6046−6054.

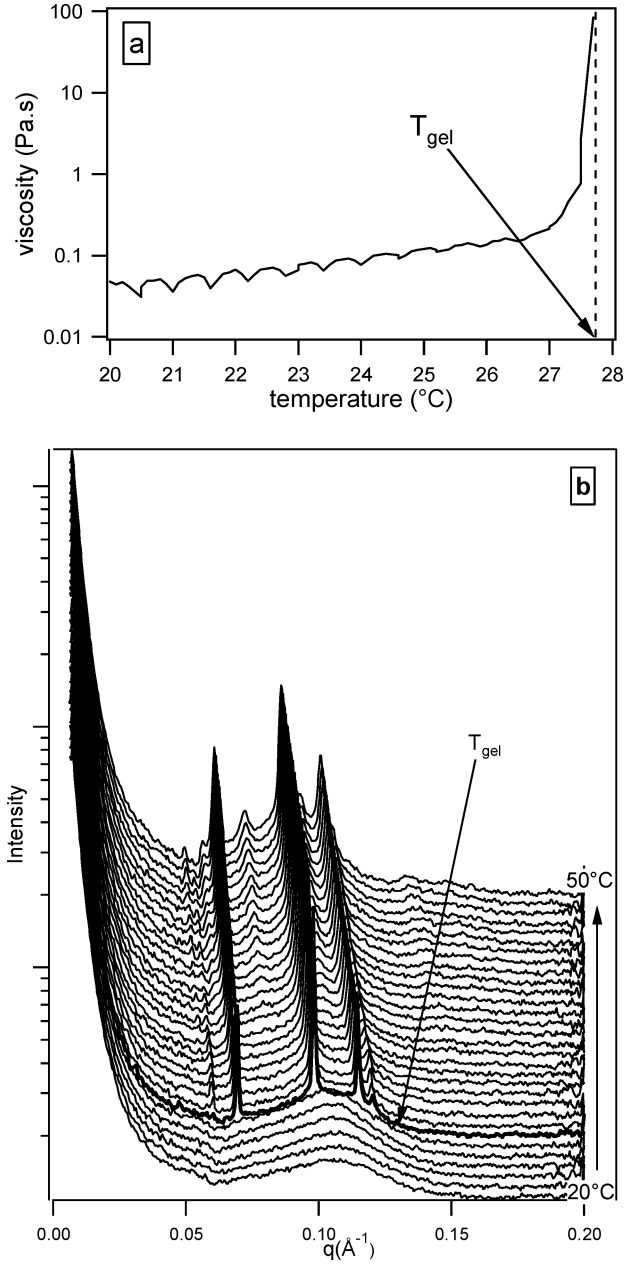

Figure 4. Determination of T_{gel} using (a) variations of the viscosity of the P85 aqueous solution, $C = 30\%$ (w/w), versus temperature and (b) X-ray profiles of the P85 aqueous solution, $C = 30\%$ (w/w), at temperatures ranging between 20 and 50 °C.

viscosity was obtained. Figure 4a displays the variation of viscosity as a function of temperature for P85 at $C = 30\%$. Figure 4b shows the evolution of the X-ray patterns for the same sample upon temperature increase. Sharp diffraction peaks appeared and grew above a temperature which was well correlated to the macroscopic formation of the gel. This experiment confirmed the already reported results that the poloxamer gelation is due to the "hard sphere crystallization of micelles".[6,36−38] The rheological measurements allowed the determination of T_{gel} as shown in Figure 4a, whereas T_{gel} could be obtained from the X-ray patterns as the temperature at which the sharp diffraction peaks appeared. The values of T_{gel} obtained by both methods are presented in Table 1. A very good agreement between both techniques was observed. SAXS and rheology are complementary, since rheology characterizes the macroscopic behavior of the sample and SAXS probes its supramolecular structure. No transition was observed on the DSC scans in the sol−gel transition

Table 1. Transition Temperatures for the Different Poloxamer Aqueous Solutions Studied

poloxamer	C (% w/w)	T_{onset} (±0.5 °C)	T_{end} (±1 °C)	T_{gel} (±1 °C)[a]	T_{gel} (±0.3 °C)[b]
F88	5	35.5	48	no gelation	no gelation
	10	31.5	44	no gelation	no gelation
	20	23.0	33	45	44.0
	25			36	33.6
	30	13.5	27	26	28.2
	35			20	22.2
P85	5	27.0	40	no gelation	no gelation
	10	21.5	35	no gelation	no gelation
	20	18.0	33	no gelation	no gelation
	25			no gelation	no gelation
	30	5.6	27	27	27.6
	35			20	22.1

[a] Gelation temperatures from SAXS experiments. [b] Gelation temperatures from rheology experiments.

Table 2. Indexation of the Cubic Phase *Im3m* of F88 in Water ($C = 35\%$ (w/w), $T = 50$ °C) with $a = 175$ Å[a]

(*hkl*)	calc q (Å^{-1})	meas q (Å^{-1})
(1,1,0)	0.0508	0.0508
(2,0,0)	0.0718	0.0719
(2,1,1)	0.0879	0.0882
(2,2,0)	0.1016	0.1018
(3,1,0)	0.1135	0.1138
(2,2,2)	0.1244	0.1247
(3,2,1)	0.1343	0.1346
(3,3,2)	0.1684	0.1689
(5,1,0) & (4,3,1)	0.1831	0.1834

[a] See also Figure 5.

Table 3. Indexation of the Hexagonal Compact Phase of P85 ($C = 30\%$ (w/w), $T = 50$ °C) with $a = 146$ Å and $c = 238.4$ Å[a]

(*hkl*)	calc q (Å^{-1})	meas q (Å^{-1})[b]
(1,0,0)	0.0497	0.0496
(0,0,2)	0.0527	0.0527
(1,0,1)	0.0562	0.0563
FCC (2,0,0)	0.0608	0.0607
(1,0,2)	0.0724	0.0723
(1,1,0)	0.0861	0.0859
(1,0,3)	0.0934	0.0932
(2,0,0)	0.0994	*
(1,1,2)	0.1009	0.1007
(2,0,1)	0.1028	*
(0,0,4)	0.1054	0.1055
(2,0,2)	0.1125	*
(1,0,4)	0.1165	*
(2,0,3)	0.1270	*
(2,1,0)	0.1314	*
(2,1,1)	0.1341	0.1334
(1,1,4)	0.1360	0.1360
(1,0,5)	0.1408	0.1408
(2,1,2)	0.1416	0.1408
(2,0,4)	0.1448	*
(3,0,0)	0.1491	0.1488
(2,1,3)	0.1534	0.1531
(0,0,6)	0.1581	0.1575

[a] See also Figure 6. [b] *: not observed.

region, denoting that gelation of F88 and P85 is an athermic process resulting from the spatial reorganization of already existing micelles. This result is in good agreement with previous studies on poloxamers.[17,27]

4. Gel Structure. The gel structure was examined by SAXS, leading to the phase assignments shown in Tables 2 and 3. Figures 5 and 6 display the SAXS profiles obtained at $T = 50$ °C for F88 at $C = 35\%$ and P85 at $C = 30\%$, respectively. Indexation of the Bragg peaks provides the space group. F88 gels exhibited

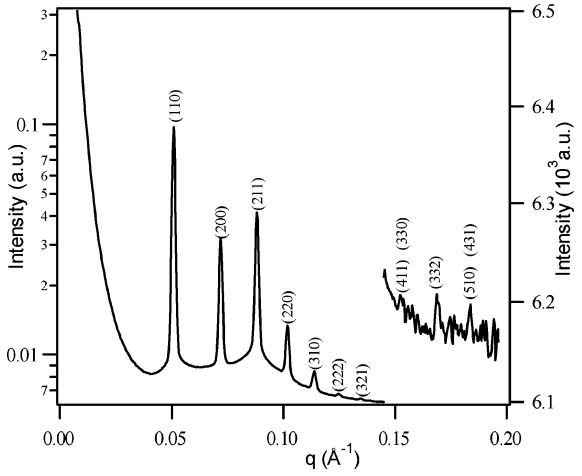

Figure 5. X-ray profile of an F88 gel at concentration $C = 35\%$ (w/w) and $T = 50$ °C in the BCC phase ($Im3m$) with $a = 175$ Å.

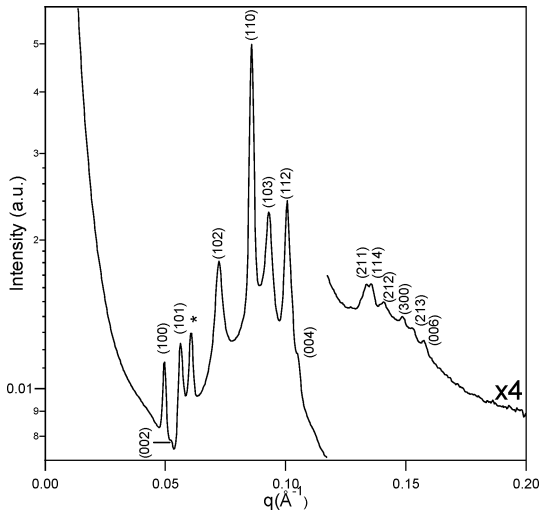

Figure 6. X-ray profile of a P85 gel at concentration $C = 30\%$ (w/w) and $T = 50$ °C in the HC phase ($P6_3/mmc$) with $a = 146$ Å and $c = 239$ Å. (*) Supplementary peak attributed to a FCC ($Fm3m$) disorder.

Bragg reflections (Table 2) in the positional ratio: $\sqrt{2}$, $\sqrt{4}$, $\sqrt{6}$, $\sqrt{8}$, $\sqrt{10}$, $\sqrt{12}$, $\sqrt{14}$, which are characteristic of a BCC structure (space group $Im3m$) with the parameter $a = 175$ Å. At $T = 50$ °C, 30 wt % gels of P85 displayed Bragg reflections (Table 3), which corresponded to a hexagonal close-packed structure, HC (space group $P6_3/mmc$), with parameters $a = 146$ Å and $c = 238$ Å. The ratio c/a is equal to $\sqrt{(8/3)}$, which means that this HC phase derives from the organization of spherical micelles.[51] However, one can note the presence of a supplementary peak in the SAXS profile (see Figure 6). This peak was attributed to the residue of a FCC (face-centered cubic) phase which was obtained with P85 samples at the beginning of crystallization ($T = 27$ °C).

5. Micelle Structure in the Gel State. From the unit cell parameters (a and c), it was possible to calculate the volume of poloxamer in a micelle, V_{pol}, according to eq 3, assuming that the polymer volume fraction, ϕ, is the same at the macroscopic and the cell levels:

$$V_{pol} = \frac{V_i}{n_i}\phi \tag{3}$$

where i = BCC, FCC, or HC, V_i is the volume of the cell, and n_i is the number of micelles in the cell. In this study, ϕ was considered to be approximately equal to C (weight/weight). For BCC, $V_{BCC} = a^3$ and $n_{BCC} = 2$; for FCC, $V_{FCC} = a^3$ and $n_{FCC} = 4$; and for HC, $V_{HC} = (6a^2c\sqrt{3})/4$ and $n_{HC} = 6$. It was then possible to extract the aggregation number, N_{ag} (i.e., the average number of poloxamer molecules per micelle), from V_{pol}, the poloxamer density, ρ (ρ was assumed to be $\sim$1 g/cm^3), and the poloxamer molecular weight, M (eq 4):

$$N_{ag} = \frac{V_{pol}\rho N_A}{M} \tag{4}$$

where N_A is the Avogadro constant.

Assuming a well-defined interface between the shell of PEO and the core of PPO in the micelle, we successively calculated the volume, V_{core}, the radius, r_{core}, and the surface, S_{core}, of the hydrophobic core and then the area per PEO block at the core−shell interface, S_{PEO}:

$$V_{core} = V_{pol}\phi_{PPO} \tag{5}$$

$$r_{core} = \left(\frac{3V_{core}}{4\pi}\right)^{1/3} \tag{6}$$

$$S_{core} = 4\pi r_{core}^{\ 2} \tag{7}$$

$$S_{PEO} = \frac{S_{core}}{2N_{ag}} \tag{8}$$

In eq 5, ϕ_{PPO} was approximated by the PPO weight fraction in the poloxamer molecule ($\phi_{PPO} = 0.21$ and $\phi_{PPO} = 0.49$ for F88 and P85, respectively). R_{hs}, the hard sphere radius, was defined as half the distance between the center of the two closest micelles in the cell. The results of these different calculations are presented in Table 4. It is interesting to note that the R values obtained in the micellar solutions (see paragraph 2) are close to the R_{hs} values obtained in the gel state (see Table 4). It thus confirms that, in the micellar solution, the scattering objects are the micelles dispersed in water.

6. F88/P85 Mixtures in Water. Mixtures with various ratios of F88 and P85 were prepared in water at a total polymer concentration $C = 30\%$. Their gelation was investigated by rheology and SAXS as previously done for the simple systems. Figure 7 displays the variation of T_{gel} as a function of the F88 weight percentage in the mixture at a total polymer concentration $C = 30\%$ in water. The gelation temperature did not vary linearly with the mixture composition and presented a maximum for an approximate F88/P85 ratio of 25/75. Although more data are needed to better define this maximum, we can emphasize that the gelation temperature was enhanced by more than 10 °C with respect to the gelation temperatures of the parent poloxamers. The results of the SAXS study performed on the mixtures (structure, cell parameters, structural parameters of the micelles) are given in Table 5. In the derivation of these parameters from eqs 3 to 6, we made the assumption that the micelles were mixed micelles as suggested by the studies of Gaisford et al.[43] and Chu et al.[44]

7. General Discussion. *Micellization and Gelation of the Pure Systems in Water*. Figures 8 and 9 display the variations of T_{onset},

(51) Guinier, A. *X-Ray Diffraction in Crystals, Imperfect Crystals and Amorphous Bodies*; Dover Publications: New York, 1994.

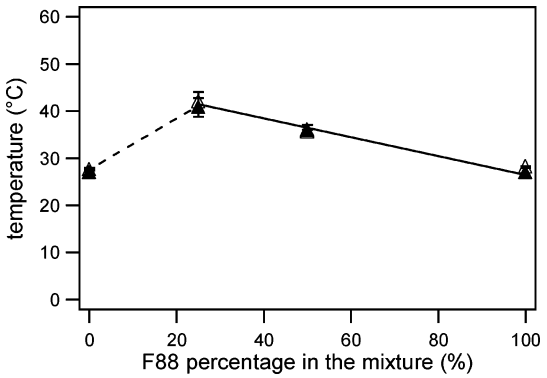

Figure 7. Variations of T_{gel} determined by rheology (△) and SAXS (▲) versus F88 weight percentage in the F88/P85 mixture at a total polymer concentration $C = 30\%$ (w/w) in water.

T_{end}, T_{gel} as a function of polymer concentration for F88 and P85, respectively. Upon temperature increase, micellization is a progressive process which takes place over more than 10 °C for F88 and 15 °C for P85. Micellization is followed by gelation provided the polymer concentration is high enough to allow sufficient micellar interactions. No gelation of P85 samples was observed in the temperature range investigated (0−50 °C) for concentrations below 30%. For F88, gelation was obtained for $C = 20\%$ and above. Importantly, for intermediate poloxamer concentrations, micellization and gelation are consecutive and not simultaneous phenomena upon temperature increase. Indeed, as shown before, the micelle radius and number increase with temperature. Micelle crystallization can only occur when the micelle radius and number are high enough to allow sufficient micellar interactions. Yet, T_{gel} approaches T_{end} upon concentration increase (especially for P85) because micelles become closer and can interact more easily.

Influence of Poloxamer Structure on the Geometrical Characteristics of Micelles. P85 exhibits higher aggregation numbers than F88 (see Table 4): at $T = 50$ °C, $N_{ag} \sim 50$ for F88 whereas $N_{ag} \sim 90$ for P85. This difference of micellar structure can be explained by geometric packing considerations. F88 and P85 have the same hydrophobic PPO block, which results in quite similar micelle hydrophobic cores ($r_{core} \sim 40$ Å for both poloxamers). Yet, the PEO blocks of F88 are 3.6 times longer than those of P85. The headgroup area of F88 is larger, and consequently, the steric constraints lead to a lower aggregation number. This effect, which is classically observed with shorter surfactant molecules, is also evidenced by the values of S_{PEO} (see Table 4). At $T = 50$ °C, S_{PEO} is approximately 130 and 160 Å^2 for P85 and F88, respectively. These different packing properties explain the different structures obtained in the gel state. In the micelles, P85 chains are densely packed, leading to "hard sphere" interactions between micelles and to a highly compact crystal structure (HC). On the other hand, F88 micelles have a soft outer shell of PEO chains and crystallize in a less compact BCC phase.

Influence of Temperature and Concentration on the Micelle Structure. The comparison of the structural parameters obtained at T_{gel} and at $T = 50$ °C for both poloxamers (see Table 4) clearly demonstrates a higher sensitivity of P85 to temperature. For instance, the aggregation number varies between 58 at $T = 27$ °C (T_{gel}) and 87 at $T = 50$ °C for P85 ($C = 30\%$), whereas it remains close to 50 for F88 ($C = 35\%$) in the 20−50 °C temperature range. This effect is most likely due to the higher proportion of hydrophobic PO units in P85 (higher ϕ_{PPO}). On the other hand, the aggregation number does not seem to vary with concentration in the concentration range investigated.

Phase Diagram of the F88/P85 Mixtures in Water. Figure 10 displays the phase diagram obtained with the F88/P85 system in water. Interestingly, whereas the aggregation number of the F88/P85 mixed micelles seems to be dominated by the influence of P85 (see Table 5), mixed micelles organize themselves according to a BCC phase in the same way as F88 alone in water

Table 4. Cell and Structural Parameters of Micelles in the Gel State for Poloxamers in Water

	ϕ	phase	a (Å)	c (Å)	V_{pol} ($\times 10^3$ Å^3)	N_{ag}	V_{core} ($\times 10^3$ Å^3)	r_{core} (Å)	S_{core} ($\times 10^2$ Å^2)	S_{PEO} (Å^2)	R_{hs} (Å)
F88 at T_{gel}	0.20	BCC	202		824	46	173	35	150	163	87
	0.25	BCC	186		804	45	169	34	148	165	81
	0.30	BCC	176		818	46	172	34	149	164	76
	0.35	BCC	174		922	51	194	36	162	157	75
F88 at $T = 50$ °C	0.20	BCC	205		862	48	181	35	155	161	89
	0.25	BCC	190		857	48	180	35	154	161	82
	0.30	BCC	182		904	50	190	36	160	158	79
	0.35	BCC	175		938	52	197	36	164	157	76
P85 at T_{gel}	0.30	HC (FCC)	128	209	445	58	218	37	175	150	64
	0.35	HC	122	200	451	59	221	38	177	150	61
P85 at $T = 50$ °C	0.30	HC	146	239	662	87	324	43	228	132	73
	0.35	HC	140	228	677	89	332	43	232	131	70

Table 5. Cell and Structural Parameters of the Mixed Micelles for the F88/P85 Mixtures in Water in the Gel State ($\phi = 0.30$)

	F88 (%)	phase	a (Å)	c (Å)	V_{pol} ($\times \mathbf{10}^3$ Å^3)	N_{F88}[a]	N_{P85}[a]	N_{ag}	V_{core} ($\times \mathbf{10}^3$ Å^3)	r_{core} (Å)
F88/P85 at T_{gel}	0	HC (FCC)	128	209	445	0	58	58	218	37
	25	BCC	172		763	11	75	86	321	42
	50	BCC	172		763	21	50	71	267	40
	100	BCC	176		818	46	0	46	172	34
F88/P85 at $T = 50$ °C	0	HC	146	239	662	0	87	87	324	43
	25	BCC	177		832	12	82	94	349	44
	50	BCC	182		904	25	59	84	317	42
	100	BCC	182		904	50	0	50	190	36

[a] N_{F88} and N_{P85} are the average numbers of F88 and P85 molecules, respectively, in a mixed micelle assuming that the proportion between the two polymers is the same at the micellar and the macroscopic levels.

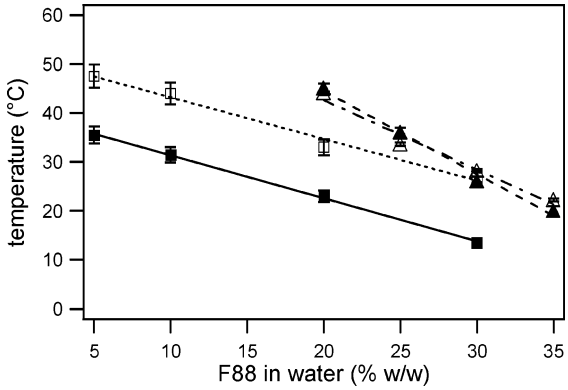

Figure 8. Transition temperatures of micellization, T_{onset} (■) and T_{end} (□), and gelation, T_{gel}, determined by rheology (△) and SAXS (▲) versus poloxamer concentration (w/w) for F88 aqueous solutions.

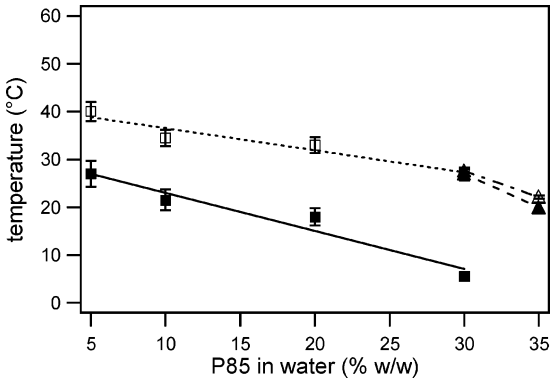

Figure 9. Transition temperatures of micellization, T_{onset} (■) and T_{end} (□), and gelation, T_{gel}, determined by rheology (△) and SAXS (▲) versus poloxamer concentration (w/w) for P85 aqueous solutions.

even when P85 is the major component of the mixture (25/75 F88/P85). Obviously, the longer PEO blocks of F88 impose their steric constraints and define softer interactions between-micelles. We observe the destabilization of the HC phase of P85 in favor of the BCC phase upon addition of small amounts of a poloxamer having the same hydrophobic PPO part but longer PEO blocks. This destabilization is accompanied by an increase of gelation temperature. It thus appears that the composition of these mixtures is an alternative way to modulate the gelation temperature around body temperature when the polymer concentration remains constant, which is interesting for pharmaceutical applications. It is noteworthy that Mortensen et al.[36,37] did not observe a HC phase for P85 gels, but they reported a BCC structure. According to our own results on the binary mixtures, this might be explained by the presence of small amounts of higher molecular weight impurities in their P85 sample (from

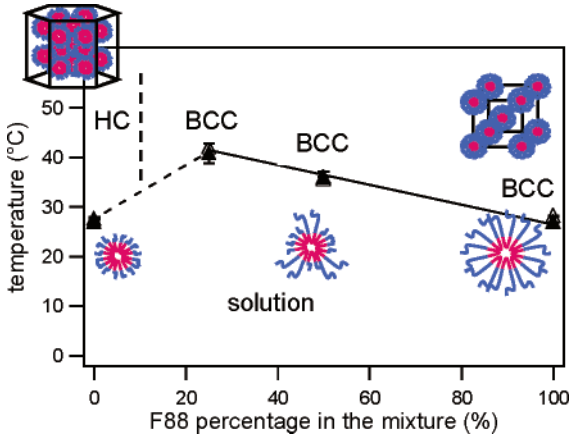

Figure 10. Phase diagram obtained with the F88/P85 system in water. T_{gel} determined by rheology (△) and SAXS (▲).

a different supplier than ours) that would cause the destabilization of the HC phase in the same way as F88 did.

Conclusion

The micellization and the gelation of two poloxamers (F88 and P85) in water were studied by the conjoint use of DSC, SAXS, and rheology. These techniques gave complementary descriptions of the systems. Micellization was mainly characterized by DSC, whereas gelation was studied by SAXS, which probed the supramolecular organization within the sample, and rheology, which characterized its macroscopic behavior. It appeared that micellization was a progressive process upon temperature increase, which was followed by gelation for sufficiently concentrated samples. Rheology and SAXS allowed the determination of the gelation temperature with a very good agreement. The temperature-induced gelation was due to the organization of poloxamer micelles under a BCC phase for F88 and a HC phase for P85 as evidenced by SAXS experiments. The radius of the micelles as well as the aggregation numbers could be extracted from the SAXS intensity profiles. Mixtures of F88 and P85 in water were also studied, and it was shown that the gelation temperature of the poloxamer mixtures was enhanced by more than 10 °C with respect to the gelation temperatures of the parent copolymers. Besides, the HC phase of the P85 gel was destabilized upon addition of small amounts of F88. This latter copolymer with its larger PEO blocks imposed its phase behavior to the F88/P85 mixture in water. Mixture composition is thus an alternative method to modulate the gelation temperature and gel structure when the poloxamer total concentration remains constant. We now intend to correlate these structural features with the diffusivities of model drugs within the poloxamer gels.

LA062622P